Noise from Arctic Ocean earthquakes

Ruth E. Keenan[a] and Ira Dyer
Department of Ocean Engineering, Massachusetts Institute of Technology, Cambridge, Massachusetts 02139

(Received 1 July 1983; accepted for publication 23 November 1983)

Earthquakes along the mid-Arctic ridge radiate earthborne compressional and shear waves, which in turn excite the Arctic acoustic channel. These waterborne arrivals, called *T* waves, have been observed about 300 km from the source and apparently enter the acoustic channel by scattering of vertical rays into nearly horizontal ones by the Arctic ice canopy above the source. The *T* waves are acoustically energetic (up to 400 kJ), are of surprisingly long duration (up to 72 s at its 8-dB down levels), have low-frequency content (peaks in the 5–15-Hz region), and have haystack spectra (4th power positive and negative dependence below and above the peak frequency, respectively). Characteristics of these sporadic noises are displayed for one event in a sonogram, in short time frequency spectra, in a time series, and in directional spectra. Directional analysis was accomplished with use of a large (~1 km) two-dimensional horizontal array. Speculations on duration of the observed events suggest that source depth, water-column reverberation above the source, and source magnitude, including "rapid-fire" multiple source excitations, could be the primary causes.

PACS numbers: 43.30.Nb, 43.30.Gv, 92.10.Vz, 93.30.Li

INTRODUCTION

In April and May 1980 sporadic acoustic events in the Arctic Ocean were observed during the Fram II experiment. This experiment made use of a horizontal hydrophone array, located approximately 300 km west of the mid-Arctic Ridge. This ridge is the locus of earthquakes which we believe create the events. The recorded events were tens of seconds in duration and quite intense, yet none was recorded by the world seismic network implying the sources were less than magnitude four earthquakes. For brevity we identify these sources as earthquakes, although such low magnitude ones are usually called microearthquakes.

The observed events are dominated by the waterborne acoustic arrival, called the *T* wave (tertiary wave), which is generated at the epicenter, i.e., above the earthquake source. The crustal arrivals are much weaker (see Fig. 1 for arrival structure). Four criteria were used to classify observed events as caused by earthquakes: (1) Did the sonogram of the event display characteristic *T* wave features? (2) Are the phase speeds of the event consistent with an earthquake model? (3) Is the time interval between the earthborne compressional arrival, known as the *P* wave (primary wave), and the waterborne *T* wave consistent with the distance to the mid-Arctic ridge? (4) Does the bearing of the *T* wave indicate a mid-Arctic ridge source with a range consistent with that calculated from the time interval between the *P* and *T* waves?

The Arctic Ocean is an excellent place to observe earthquake events, in part because of its low-frequency transmission stability[1] and low-ambient noise[2] and in part because the ice cover at the epicenter appears to scatter sound effectively into the acoustic channel. Although delayed to a later study, the ice scattering function could be measured from the observed *T* wave by modeling the earthquake source (earthquakes of known magnitude and focal depth may be required).

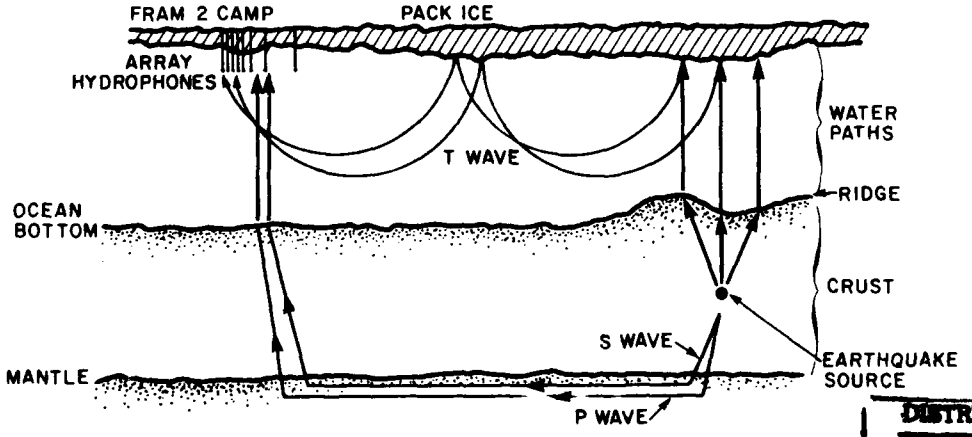

FIG. 1. Scheme of seismic and acoustic propagation from an earthquake. Vertical scale grossly exaggerated (ice thickness about 3 m, water depth about 4 km, crust and sediment thickness about 10 km, distance between source and array about 300 km, slopes of mid-Arctic ridge less than 2°). The nearly vertical bundle of rays at the epicenter (above the earthquake) determines the acoustic source diameter and its minimum time-width in propagation past the array.

[a] Permanent affiliation: Science Applications, Inc., P.O. Box 721, Woods Hole, MA 02543.

 0001-4966/84/030819-07$00.80

I. DATA ACQUISITION AND PROCESSING

Fram II was conducted in deep water on an ice floe over the western edge of the Pole Abyssal Plain in the eastern Arctic (Fig. 2). Ambient noise, backscattering, transmission loss, and reflection and refraction profiles were measured. The array (see Ref. 3, for array layout) was composed of 24 hydrophones, spaced logarithmically, and suspended 91 m in the water through holes drilled in the ice. Initially the array was an L shape 1.2 km on a side. Due to ice break up, however, the array was reconfigured on 16 April 1980 to a cross 800 m on a side. The array position on 11 April 1980 for the first of our events was 86°24′ N and 22°12′ W. It drifted to 85°54′ N and 25°07′W by 1 May 1980 for the last of our events. The acoustic data, recorded by a 24 channel data acquisition system at a 4-ms sampling rate on 9-track magnetic tapes, had a useful frequency range between 1 and 80 Hz. Over 407 h of data were recorded by the array. The system characteristics are described by Prada *et al.*[4]

The search for earthquake events among the data tapes was simplified by Lamont Doherty Geological Observatory's participation in Fram II. Kutschale *et al.*[5] had geophones set up on the ice which continuously monitored seismic activity. By listening to their analog records they noted the times of 32 events (see Ref. 5). Of these, five occurred while the hydrophone array data were being recorded. It is these five events that are reported upon here.

II. DATA INTERPRETATION

One can visualize the physical situation quite simply. Waves radiate from an earthquake source through the crust and mantle to the receivers. When remote from the source the first arrival will be the crustal P wave that couples to the mantle and travels as a head wave at the mantle speed.[6] This speed was measured during Fram II by refraction profiling and is about 8 km/s.[3] Other waves follow the head wave at speeds given by the crustal compressional wave speeds. Each of these has a corresponding shear wave, known as an S wave (secondary wave). The first S wave, corresponding to the head wave, will have a speed of about 5 km/s according to the foregoing authors. The T wave travels in the acoustic channel and arrives thereafter (these P, S, and T waves are sometimes called P, S, and T phases, respectively, especially in the literature of seismology. It seems more appropriate to use the former for an acoustics audience for whom the word "phase" has a particular meaning not at all intended by seismologists, some of whom now use the description "wave").

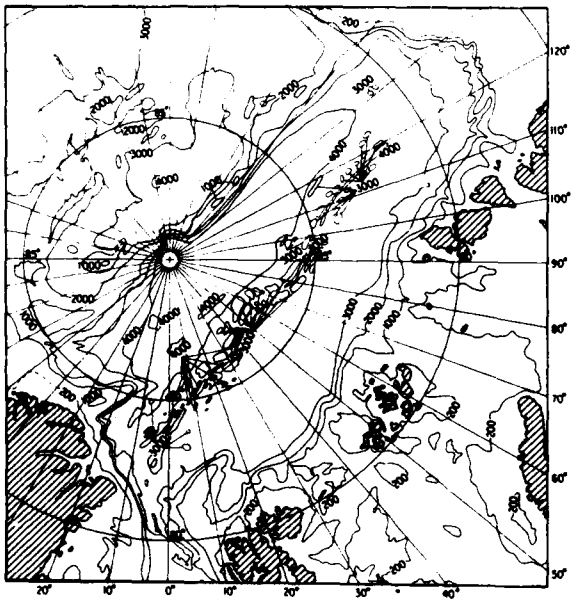

FIG. 2. Major features of the eastern Arctic Ocean. The FRAM II camp was located at 86.4° N, 22.2° W at the beginning of the observations reported herein, and at 85.9° N, 25.1° W at the end. The mid-Arctic ridge or spreading center runs from about 83° N, 5° W to about 81° N, 120° E. For orientation, the NE coast of Greenland (about 83° N, 20° W), the North coast of Svalbard (80° N, 20° E), and the North coast of Severnaya Zembya (82° N, 95° E) are useful. Depth contours in meters. Redrawn from Canadian Hydrographic Service.[14]

To model the T wave, consider the ensonified region on the sea floor centered on the earthquake source. This region transmits acoustic waves nearly vertically into the water column. To propagate in the Arctic RSR channel it must be converted to ray angles less than about 20° from the horizontal. There are two conversion possibilities: first, scattering by the upper boundary formed by the rough ice canopy and second, refraction into horizontal directions by the rough water/bottom interface. The former is well-coupled to the Arctic acoustic channel and the latter is not because of its depth (Fig. 2). (While the conversion mechanism is of interest, it is not relevant to the main thrust of this paper.)

Duennebier[7] noted that the peak frequency arrival, f_m, of a T wave travels roughly at the average water column speed, c_w, in this case 1.47 km/s. Note that f_m simply is the highest frequency ascribed to the event, and of course is somewhat arbitrary in that its value is signal/noise dependent. But it is useful as a single mark for arrival time of the T wave. The range R to the source thus can be estimated by the time difference, Δt, between the P wave traveling at the mantle speed, c_p, and the T wave traveling at c_w as follows:

$$\Delta t \approx R\,(1/c_w - 1/c_p). \tag{1}$$

In Eq. (1) we have neglected travel time and refraction in the crust. These account for about a 2-s error in Δt which totals about 160 s. We have also neglected the 1–3 s time spreading expected for the Arctic RSR channel.[8]

III. DATA

For each event (1) a time series, (2) frequency spectra, (3) a sonogram, (4) a bearing diagram, and (5) a phase speed spectrum were constructed. This set is shown for one event in Figs. 3–8. The time series is displayed as a stack or composite of many channels from a few seconds before the event until after the event has terminated. The shape of the pattern formed by stacking the signals (the moveout) reflects the orientation of the two orthogonal legs of the array and the vertical arrival angle of the waves. The frequency spectra are formed from a 2-s data sample from noise prior to and during the event. Stacking of such data forms the sonogram of the entire event; the contour levels of the sonogram are referenced to the measured peak spectral level. The bearing and

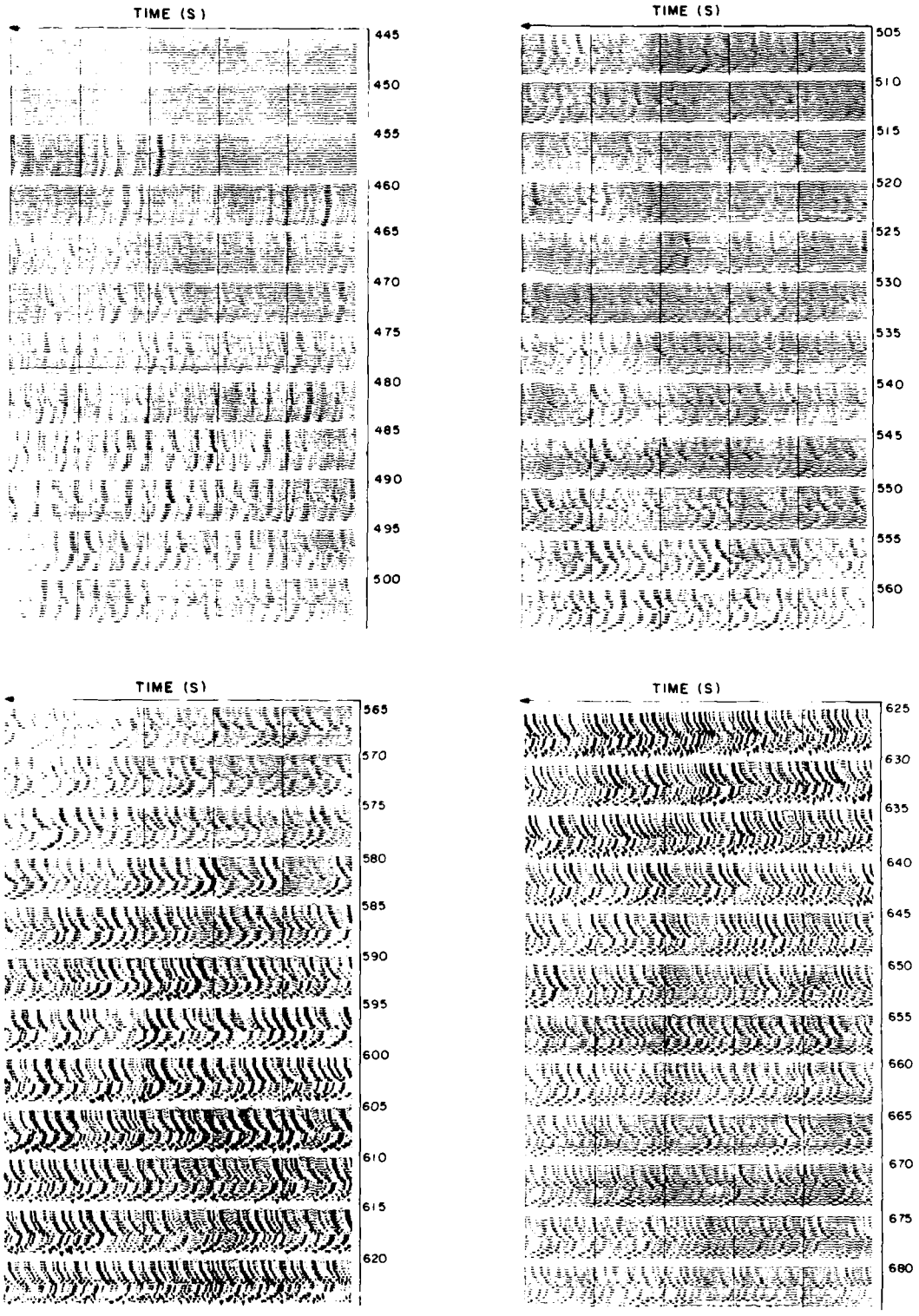

FIG. 3. Time series of tape 5042 from 445–685 s. Channels 1–4, 6–10, 13–16, and 18–20 in ascending order.

speed spectra are obtained with use of the directional properties of the array and maximum-likelihood-method processing.[9,10,11] The bearing plot is based on 2-s data samples using 2-Hz bandwidths centered on 16 Hz and the speed spectrum plot on 0.5-data samples using 2-Hz bandwidths centered on 5 Hz.

The event of Figs. 3–8 was recorded at a tape-start time of 03:09:37 Z on 14 April 1980. The first arrival in the time

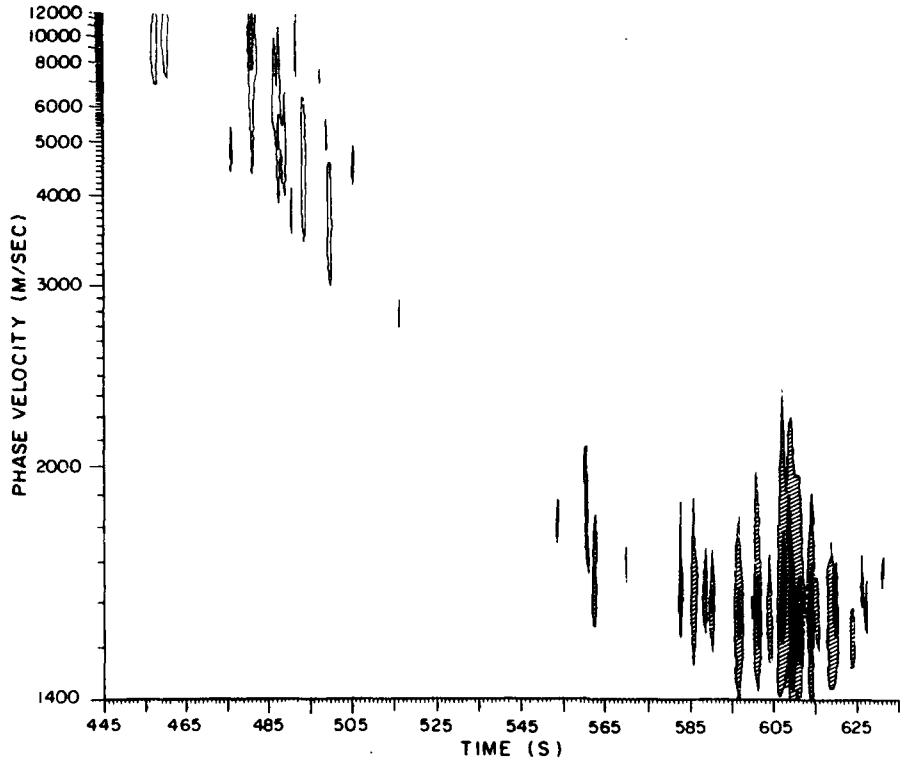

FIG. 4. Vertical directionality (phase speed spectrum) at center frequency 5 Hz, bandwidth 2 Hz, time window 2 s. The relative contour levels are 5 dB apart, extending from filled (highest) to unfilled (lowest).

series (Fig. 3) is presumably the head wave, which rises sharply out of the background noise at 457 s (time is referenced to the start of the data tape). There is very little moveout among channels for these initial arrivals, consistent with nearly vertical rays, i.e., crustal arrivals. From 550–660 s a set of arrivals with more moveout grows and decays. The moveout and the time lag from the crustal arrivals suggest waterborne energy. This is verified by the phase speed spectrum (Fig. 4). The arrival at 457 s has a phase speed greater than 7 km/s and is followed by arrivals with phase speeds decreasing to 4 km/s. We expect the head wave to arrive first with a phase speed of about 8 km/s and the other crustal waves to follow with decreasing phase speeds, as the data show. The arrivals 100–200 s later have phase speeds less than 2 km/s indicative of waterborne energy, again as expected.

The spectra of 2-s samples from 1–80 Hz are presented before the event (Fig. 5) and during the event (Fig. 6). The spectral levels of the ambient noise in Fig. 5 have a shape and values commonly observed.[2] The spectrum of the T wave (Fig. 6) is quite different; it is a function of source behavior,

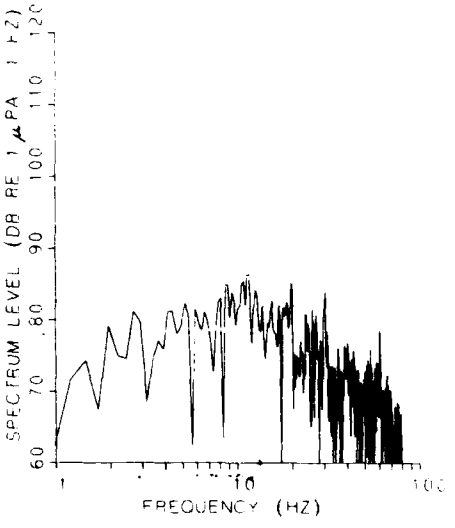

FIG. 5. Spectrum of ambient noise prior to T wave, 430–432 s. Peaks at 30 and 60 Hz are mechanical and electrical interference from the camp's motor generator.

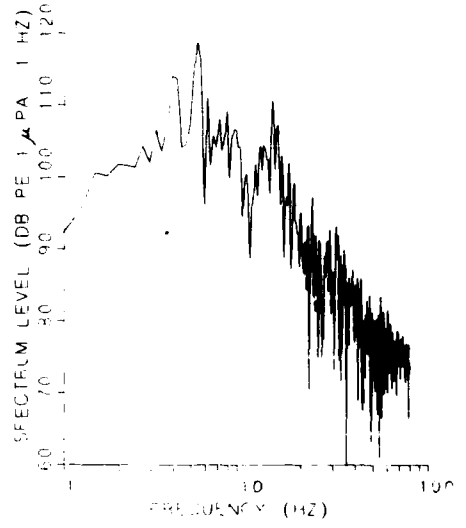

FIG. 6. Spectrum of T wave at time of peak-frequency arrival, f_m (604–606 s).

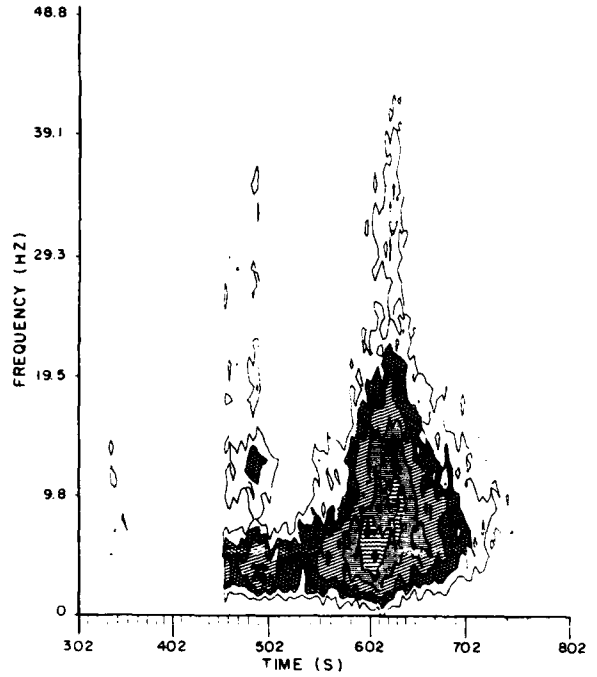

FIG. 7. Sonogram showing early P and S arrivals (>457 s) and T arrivals (550–660 s). The contour levels extend from spectrum levels of 113 dB *re*: 1 μPa and 1 Hz (filled) to 88 dB (unfilled), with various intermediate cross-hatching at 5-dB intervals. (Levels below 3 Hz are reduced by a 18 dB/oct filter with a 1-Hz loss of 8 dB.) Time-window 2 s.

ice scattering, and RSR transmission.

The sonogram (Fig. 7) displays a shape characteristic of T waves reported by Duennebier,[7] Northrop,[12] and Northrop *et al.*[13] This shape has been variously described as "tear drop," "pear," or "Christmas tree." We see that a T wave is both intense and of long duration. At $f_0 = 5$ Hz, the peak level L_p exceeds the ambient noise by 30 dB, with a duration of the contour 8 dB down from the peak level of 72 s. The time interval between the P wave and the arrival of f_m (read from the sonogram) is 174 s, which according to Eq. (1) gives $R \approx 313$ km.

The bearing of the T wave (Fig. 8) is about 099°, which according to a contemporary chart[14] intersects the rift valley at $R \approx 318$ km, in good agreement with that from the measured time difference between P and T arrivals. We see that our criteria for labeling this event as one of earthquake origin are well met.

The other four events are similar to the one presented; for comparison, relevant physical characteristics are summarized in Table I, including those for the event shown in the figures. With only five samples of 32 events the increase then decrease in L_p (item 9) cannot be deemed significant. Features such as duration (item 10), time patterns (items 11 and 12), and f_0 (item 7) seem to have no connection to the variation of L_p nor to any other characteristic. It should be said that the apparent shift in f_0 from 5–15 Hz is probably related to two different haystack spectra in each spectrum, one peaked at 5 and the other at 15 Hz (see Fig. 6). Just a slight variation of observational condition apparently can emphasize one over the other. Notwithstanding this uncertainty the spectral shapes seem to be in reasonable agreement (item 8) with a f^4 and f^{-4} low- and high-frequency dependence, respectively, as the best simple statement of the result.

Two procedures were used to estimate epicentral range [items 5(a) and 5(b)]. One [5(a)] is based on the intersection of the bearing with the mid-Arctic ridge using the Canadian Hydrographic Service map #5–17,[14] the other [5(b)] is based on the time difference between the observed P wave and peak-frequency arrival of the T wave. The estimated source initiation time (item 3) is based on the measured arrival time of the peak frequency of the T wave, corrected for the travel time in the water using the measured range [5(b)]. The estimated source location (item 4) is based on the range in item 5(b) and measured bearing (item 6). It is a somewhat more accurate determination of the source location (within ± 3 km in range and ± 10 km in azimuth) than source location determined from a map's placement of the rift valley. The source may not actually be located on the rift valley and such maps are typically accurate to only ± 10 km.[15]

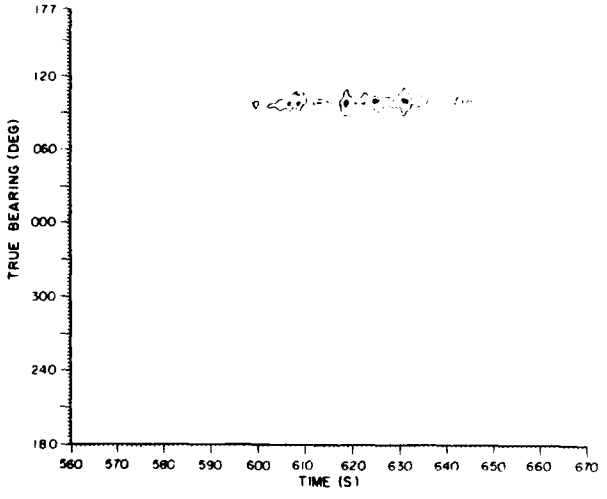

FIG. 8. Horizontal directionality at center frequency 16 Hz, bandwidth 2 Hz, time-window 2 s. The relative contour levels are 5 dB apart, with the one filled-in the higher of the two.

IV. DISCUSSION

The duration of the T wave is surprisingly long, within 26–72 s as defined by the 8-dB-down contour. Several mechanisms were considered to explain this: S wave contribution, source depth, RSR channel spreading, secondary acoustic scattering, and sloping seafloor and/or multiple bounces at the epicenter. Of these only source depth and multiple bounces were found to account for more than just a few seconds.[16] To these should be added source magnitude and its various manifestations as they may affect duration.

An earthquake ensonifies a region on the seafloor which transmits the T wave into the water. This has an inherent time spread determined by the diameter of the ensonified region, i.e., the time difference between the leading and trailing edge propagating past the receiver. Johnson *et al.*[17] found they could significantly vary duration with use of such a model by adjusting the source depth. They assume lossless

TABLE I. Summary of array processed seismic events from the FRAM II experiment.

1.	FRAM II tape	2002	5030	5042	2021	5373
2.	Date	11 April	13 April	14 April	17 April	1 May
3.	Estimated source initiation (h:m:s) $\pm$ 2 s	14:50:16[c]	21:50:17	03:08:58	22:51:46	04:30:16
4.	Estimated source location (°N: °E)	84°07′ 0°27′	84°45′ 5°02′	85°06′ 12°22′	84°39′ 2°33′	84°30′ 3°10′
5(a).	Map epicentral range ($\pm$ 10 km)	324	299	318	311	297
5(b).	Data epicentral range ($\pm$ 3 km)	b	292	313	294	301
6.	True bearing (deg) $\pm$ 2°	129	114	099	117	106
7.	Frequency of spectral peak f_0 (Hz)	5	5	5	15	15
8.	Spectral shapes at low and high frequencies ($f^m : f^{-n}$)	m[a] $n \sim 3\frac{1}{2}$	$m \sim 3\frac{1}{2}$ $n \sim 4$	$m \sim 3$ $n \sim 4$	$m \sim 5$ $n \sim 4\frac{1}{2}$	$m \sim 4$ $n \sim 4\frac{1}{2}$
9.	Level of spectral peak L_p (dB *re*: 1 μPa, 1 Hz)	103	105	116	119	105
10.	Duration of 8-dB contour (s)	38	26	72	26	56
11.	Time of f_0 arrival *re*: center of 8-dB contour (s)	− 15	− 3	− 10	− 5	+ 10
12.	Time of f_m arrival *re*: center of 8-dB contour (s)	0	+ 2	+ 17	− 2	+ 10

[a] Hydrophone strum dominated signal.
[b] No data.
[c] Estimated using item 5(a).

spherical spreading from a monopole source and get the relative power level L

$$L = 10 \log[h^2/(h^2 + R_0^2)], \tag{2}$$

where h is source depth below the seafloor, and R_0 the horizontal range of the ensonified region. We have no *a priori* information on source depth for our events but in general $h \leqslant 10$ km[15,18] for mid-ocean ridges. For a 10-km source depth, the diameter of the 8-dB-down contour is less than 46 km and the duration less than 31 s. Thus source depth could explain duration at one extreme of the observations (26 s) but not at the other (72 s). We emphasize that 31 s is an upper limit for source depth effect, not only because it corresponds to the largest reasonable depth (10 km) but also because it ignores absorption of P and S waves in the crust, which tends to limit the diameter of the 8-dB contour.[16]

Equation (2) is based on a monopole model. Keenan[16] adopted a quadrupole model for earthquake radiation[6] but, for a wide range of assumptions on source orientation, found the conclusion basically unchanged: source depth affects the duration significantly, but not enough to account for all observations.

Multiple bounces in the water/bottom column at the epicenter can also affect the duration. Abbot[19] studied multiple reflections for signals at near normal incidence in the Arctic. He found the average coherent loss per bounce for frequencies less than 30 Hz to be 6 dB. It is likely that the incoherent loss is no smaller than 3 dB per bounce. Using the optimistic incoherent loss figure we estimate no more than three bounces could contribute energy within the 8-dB-down contour. In our case, water column multiples are about 3–5 s apart, based on known bathymetry of the ridge. By including a 10-km thick crust with an average 5 km/s speed[3] multiples also could occur every 7–9 s. If we attempt to make up the difference between the longest observed event (72 s) and the deepest possible source (31 s) with multiple bounce time-spreading, we would need more vertical multiples than Abbot's data suggest are possible. Hence we conclude that while multiple bounce can be important, possibly accounting for up to about 27 s of time spreading within the 8-dB contour, it cannot explain all observations.

We come now to source magnitude considerations, which can influence duration as well as peak values. The energy radiated by a single earthquake slip is[6]

$$E = \eta A l \tau, \tag{3}$$

where η is a fixed fraction of total energy which radiates, the remainder being invested in work as the two slip planes grind against each other, A is the slip plane area, l the average slip length, and τ the resolved slip plane stress. While τ is not likely to be a constant, we can assume its range of values to be small with respect to variations in the other parameters.[15]

This energy radiates in the time interval T_0, which for an individual slip can be estimated as l/v, where v is the average rupture or slip speed, which Brune[20] takes as the shear speed. With shear speed about 5 km/s, we see that for a single slip T_0 is small for all but unreasonably large values of l. The observed durations cannot be explained by simple application of the estimate l/v, nor by implication can we successfully use Eq. (3) to explain the observed levels. Indeed comparison of the peak level L_p in Table I with duration shows no consistent trend, in contrast to that expected from Eq. (3). For example, if A scales as l^2 (see Ref. 15) then we would have $E \sim \tau T_0^3$, but such is not observed.

There are other seismological effects relating to source magnitude which can affect duration. For example one can conceive of the total motion as slip-stick-slip, in which case both magnitude and duration are governed by the composite of many individual slips in "rapid-fire" sequence. The time series (Fig. 3) and the speed spectrum (Fig. 4) indicate high-phase speed crustal arrivals of duration long enough (~ 40 s) to account for the total duration of 72 s in combination with the other mechanisms. Whether these high-phase speeds are rapid-fire P wave events or higher order arrivals from one event cannot be discerned from the data.

As a final point we observe that an estimate of the RSR source level L (0) can be obtained from

$$L(0) = L_P + H, \tag{4}$$

where L_P is the sound pressure level measured at the receiver and H the transmission loss. A crude estimate gives $H \approx 88$ dB *re*:1 m for all events, which then yields $191 \leqslant L(0) \leqslant 207$ dB *re*:1 μPa, 1 Hz, 1 m as the range for our observed events. With the assumption of horizontal omnidirectionality, and a bandwidth estimate of 5 Hz from the data, we find the maximum acoustic power radiated into the RSR channel to range from about 0.5–20 kW, and the energy from about 10–400 kJ. While classed as microearthquakes, these seismic events can be sporadically intense acoustic sources.

ACKNOWLEDGMENTS

Many people contributed to the progress of this work. The support of John Hanna, Chuck Spofford at SAI, and Jess Stanbrough at WHOI; the data from Henry Kutschale, Tai Lee, and Charlie Monjo at LDGO; the conversations with Peter Stein, Greg Duckworth, Art Baggeroer, Nafi Toksöz at MIT, Ralph Stevens, Mike Purdy at WHOI, Anne Trehu at USGS, Charlie Votaw at NRL, and Leonard Johnson at ONR; and the data processing help of Dave Gever, Leon Schuyler, and Ken Prada at WHOI are all appreciated. Work supported by ONR.

[1]P. Mikhalevsky, "Characteristics of cw signals propagated under the ice in the Arctic," J. Acoust. Soc. Am. **70**, 1717–1722. (1981).
[2]I. Dyer, "The song of sea ice and other arctic ocean melodies," Robert Bruce Wallace Lecture, M.I.T. *Arctic Policy and Technology* (Hemisphere, New York, 1983).
[3]G. L. Duckworth, A. B. Baggeroer, and H. R. Jackson," Crustal structure measurements near FRAM II in the Pole Abyssal Plain," Tectonophysics **89**, 173–215 (1982).
[4]K. Prada, K. von der Heydt, and T. F. O'Brien, "A versatile multichannel data acquisition system for seismic and acoustic applications," in *Proceedings of the Oceans 81 Conference* (IEEE P, New York, 1981).
[5]H. Kutschale, C. Monjo, and T. Lee, personal communications (1982).
[6]K. Aki and P. Richards, *Quantitative Seismology, Theory and Methods* (Freeman, San Francisco, 1980).
[7]F. K. Duennebier, "Spectral variation of the T phase," Hawaii Institute of Geophysics Rep. HIG-68-22 (December, 1968).
[8]I. Dyer, A. B. Baggeroer, J. F. Zittel, and R. J. Williams, "Acoustic backscattering from the basin and margins of the Arctic Ocean," J. Geophys. Res. **87**, 9477–9488 (1982).
[9]A. B. Baggeroer and S. J. Leverette, "Estimating of velocity/depth spectra using the maximum likelihood method (MLM)," Soc. Expl. Geophys. Meet. (A) (1975).
[10]A. B. Baggeroer and R. K. H. Falconer, "Array refraction profiles and crustal models of the Canada Basin," J. Geophys. Res. **87**, 5461–5476 (1982).
[11]E. K. Scheer, "Estimates of crustal transmission losses using MLM array processing," thesis, MIT, Cambridge, MA (May 1982).
[12]J. Northrop, "Evidence of dispersion in earthquake T phases," J. Geophys. Res. **67**, 2823–2830 (1962).
[13]J. Northrop, M. Blaik, and I. Tolstoy, "Spectrum analysis of T phases from the Agadir earthquake February 29, 1960, 23h, 40m, 12s, GCT, 30° N, 9° W (USGCS)," J. Geophys. Res. **65**, 4223–4224 (1960).
[14]Canadian Hydrographic Service, General Bathymetric Chart of the Oceans, map no. 5–17 Ottawa (1979).
[15]R. C. Lilwall, "Seismicity of the ocean rifts," in *Continental and Oceanic Rifts*, edited by G. Palmason (Geodynamic Series), Vol. 8, pp. 63–81 (1982).
[16]R. E. Keenan, "Seismic events in the Arctic Ocean," thesis. MIT, Cambridge, MA (January 1983).
[17]R. H. Johnson, R. A. Norris, and F. K. Duennebier, "Abyssally generated T phases," in *The Crust and Upper Mantle of the Pacific Area*, Am. Geophys. Union, Geophys. Mono. **12** (1966).
[18]B. T. R. Lewis, "The process of formation of ocean crust," Science **220**, 151–157 (1983).
[19]P. M. Abbot, "Reflection losses of the Arctic Ocean bottom," thesis, MIT, Cambridge, MA (May 1979).
[20]J. N. Brune, "Tectonic stress and the spectra of seismic shear waves from earthquakes," J. Geophys. Res. **75**, 4997–5009 (1970).